TU Delft

Delft University of Technology

Automated Correction of Refraction Residuals

Beaudoin, Jonathan; Renoud, Weston; Haji Mohammadloo, Tannaz; Snellen, Mirjam

Publication date
2018

Document Version
Accepted author manuscript

Published in
HYDRO18 Conference

Citation (APA)
Beaudoin, J., Renoud, W., Haji Mohammadloo, T., & Snellen, M. (2018). Automated Correction of Refraction Residuals. In *HYDRO18 Conference: 30 October – 1 November 2018, Sydney, Australia*

Important note
To cite this publication, please use the final published version (if applicable).
Please check the document version above.

Copyright
Other than for strictly personal use, it is not permitted to download, forward or distribute the text or part of it, without the consent of the author(s) and/or copyright holder(s), unless the work is under an open content license such as Creative Commons.

Takedown policy
Please contact us and provide details if you believe this document breaches copyrights.
We will remove access to the work immediately and investigate your claim.

This work is downloaded from Delft University of Technology.
For technical reasons the number of authors shown on this cover page is limited to a maximum of 10.

Automated Correction of Refraction Residuals

Jonathan Beaudoin[1], Weston Renoud[2], Tannaz Haji Mohammadloo[3], Mirjam Snellen[3]
1. QPS Canada Inc., Fredericton, NB, Canada, beaudoin@qps.nl
2. QPS B.V., Zeist, The Netherlands
3. Technical University of Delft, Delft, The Netherlands

ABSTRACT

In a world of high precision sensors, one of the few remaining challenges in multibeam echosounding is that of refraction-based uncertainty. A poor understanding of oceanographic variability or a poor choice of equipment can lead directly to poor quality bathymetric data.

Post-processing software tools have existed for some time to allow data processors to correct for these artifacts. These tools typically involve the manual review of soundings and manual adjustment of a small set of parameters to achieve the desired correction. Though there are a number of commercial solutions currently available, they all have the same inherent weaknesses: (1) they are manual, thus time-consuming, (2) they are subjective, thus not repeatable, (3) they require expert training and thus are typically only usable by experienced personnel.

QPS and the Technical University of Delft, The Netherlands (TU Delft) have worked together to implement an algorithm to address these issues in QPS' post-processing software, Qimera. The algorithm, the TU Delft Sound Speed Inversion, works by taking advantage of the overlap between survey lines, harnessing the power of redundancy of the multiple observations. For a given set of pings, the algorithm simultaneously estimates sound speed corrections for the chosen pings and their neighbors by computing a best-fit solution that minimizes the mismatch in the areas of overlap between lines. This process is repeated across the entire spatial area, allowing for an adaptive solution that responds to changes in oceanographic conditions. This process is completely automated and requires no operator interaction or data review. The algorithm is also physics-based in that it honors the physics of acoustic ray bending. For accountability, the algorithm preserves the output of the inversion process for review, vetting, adjustment, and reporting.

In this paper, we briefly explain how the algorithm works in simple terms. We also explore two data sets that cover differing oceanographic conditions, seabed morphologies, and survey line planning geometries in order to establish some early guiding principles on how far the algorithm can be pushed for performance.

INTRODUCTION

Multibeam echosounders (MBES) collect oblique soundings, allowing for a remarkable increase in coverage compared to traditional downward looking single beam echosounders (SBES). The gain in coverage comes at a cost: the speed of sound through water varies with depth and can cause the oblique sounding ray paths to refract, introducing significant and systematic biases in soundings. This is readily corrected by measuring the sound speed variation with depth and using this additional information to model the acoustic ray path using acoustic ray tracing techniques. Since the speed of sound in water is determined primarily by temperature and salinity, any significant spatio-temporal variations of these two quantities can significantly change the sound speed structure and can lead to sounding biases if an unrepresentative sound speed profile (SSP) is used for refraction correction. The hydrographic surveyor must then take care to sample often enough to capture the important changes in the water mass such that refraction type biases are avoided. This is typically done by stopping the survey vessel to collect a SSP by lowering a Conductivity-Temperature-Depth (CTD) sensor or a velocimeter sensor. There are also solutions that allow SSPs to be collected while underway, allowing for an increase in efficiency. Despite best efforts by surveyors to adequately measure the water mass variability, it sometimes occurs that insufficient measurements are collected, resulting in systematic biases in MBES results. These biases take on the form of so-called “smile” or “frown” artifacts across the MBES angular sector, with the outer soundings curling either upward or downward, respectively.

Previous efforts to address this type of problem have been proposed, largely in post-processing. The reader is directed to Mohammadloo et al. (2018) for a brief synopsis discussion of these methods, and of course the original works. We provide a short list here for the interested reader:

- Kammerer and Hughes Clarke (2000)
- Ding et al. (2008)
- Jin et al. (2016)

In this contribution we propose a method for estimating the sound speed and bathymetry that fully employs the redundancy of the overlapping MBES swaths between adjacent survey lines. Given that there is standardly at least a small amount of overlap between adjacent passes, the same spot on the seafloor in the corridor of overlap will thus be imaged by two independent passes. The expectation is that the depth measurement results from the two passes are consistent. Assuming that all other sources of uncertainty are well controlled (including vertical positioning), a discrepancy in the resulting depth measurements is often due to the water column oceanographic conditions fluctuating at a rate higher than the surveyor is sampling it.

Sound speeds are estimated for a pseudo-model of the water column by minimizing the difference between the water depths in the overlapping parts. This method provides (1) the bathymetry for which the errors due to an insufficient knowledge about the sound speeds have been diminished and (2) information about the water column sound speeds itself.

METHODOLOGY

In this section, we quickly explain the basic functioning of the proposed SSP inversion algorithm. Assume that the MBES measurements are acquired such that an overlap exists between adjacent swaths. Figure. 1a shows MBES survey geometry, consisting of four tracks that have been sailed parallel to each other with a certain percentage of overlap. The MBES measurements consist of measured two-way travel times for all beams across each of these swaths and the depths are derived by rotating the beam vector from the transducer frame to the navigation frame. An example of the effect of using erroneous SSPs on the estimated water depths is shown in Figure. 1b, see the depth differences at the overlapping parts.

For a well-calibrated MBES (known mounting offsets) with a good control on the vertical positioning, one can attribute the observed difference in the water depths at the overlapping parts to the use of incorrect information regarding the SSP.

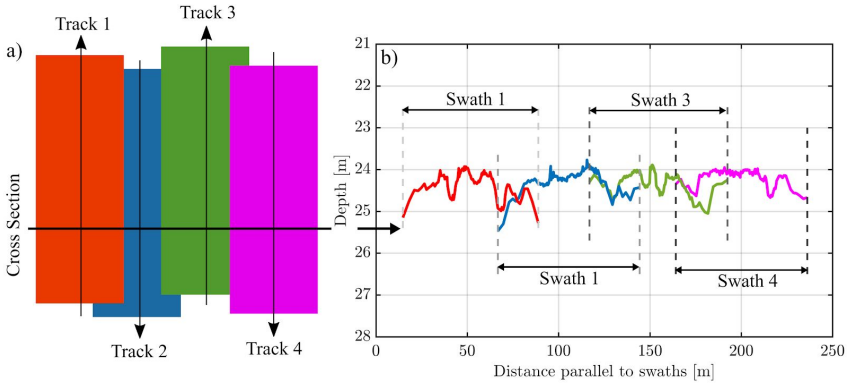

Figure 1. a) Schematic of survey configuration. The arrows indicate the sailing direction, b) Example of differences in estimated bathymetry at overlapping swaths due to insufficient information about the water column sound speed.

In the proposed method, sound speeds are sought which maximize the agreement in water depths at overlapping parts of the swaths. Due to the varying MBES time and position for each of the swaths sound speeds can differ from track to track, thus, if there are *N* track lines for the segment under consideration, *N* unknown SSPs parameters should be searched for. The energy function is defined as

$$E(\mathbf{x}) = \sum_{c=1}^{C} \sqrt{\frac{\sum_{n=1}^{N} \sum_{b=1}^{B_{c,n}} (z_{c,n,b}(\mathbf{x}) - \bar{z}_c(\mathbf{x}))^2}{\sum_{n=1}^{N} B_{c,n}}} \qquad (1)$$

C is the number of grid cells in the segment considered and $B_{c,n}$ is the number of soundings in a cell (c), for the given track (n). $z_{c,n,b}$ is the depth of a sounding for the given cell, track and beam (b) and z_c is the weighted mean of $z_{c,n,b}$ with the weight function being the inverse cubed horizontal distance between the sounding and cell center. $z_{c,n,b}$ are recalculated using the new estimate of the SSPs. If a uniform sound speed within the water column is considered, **x** contains N unknown sound speeds for the segment under consideration.

Optimization of E (minimization of the energy function) yields to the sound speeds resulting in a maximum agreement between water depths along different swaths at overlapping points. Locating the minimum of Eq. (1) is carried out using the Differential Evolution (DE), see Snellen and Simons (2008), which is a global search algorithm (Price and Storn, 1995).

Using DE for the optimization allows for an arbitrary SSP parameterization. However, it requires a significant number of forward calculations. To reduce the computational effort of the method, Gauss-Newton (GN) can be used for the optimization instead of DE. As discussed, the DE optimization searches for each track's SSPs. For GN, both SSPs and water depths are considered as unknown and the energy function is defined as the sum of the square of the differences between measured and modelled two way travel times, see Snellen et al. (2009). The modeled two way travel time accounts for the effects of the sound speed on the beamsteering and propagation through the water column. Each cell in the overlapping part is assumed to be a plane with the normal vector of [0, 0, 1]. The two way travel time is derived using the intersection of the line passing through the transducer position and a given beam in a given track and the plane, see Mohammadloo et al. (2018). The unknown parameters (sound speeds of the tracks in the overlapping part and cells depths) can be derived using Least Squares method, see Teunissen (2000).

CASE STUDY ANALYSIS

Assessment Methodology

To assess the performance of the SSP inversion method, we decided to use a high quality data set without any refraction issue and to investigate whether the method is capable of reproducing the original surface if an incorrect SSP is applied to the original data instead of the correct SSP acquired using data acquisition. Essentially, we take good data and intentionally introduce a refraction artifact and then we see if the inversion algorithm can repair the data by comparing it to the original results. To this end, the dynamic surface derived from the original data is compared to that of derived after the application of the SSP inversion. Ideally, both surfaces have to be similar and the bottom morphology has be intact. Moreover, the result of the algorithm has to be unbiased. This means that if the SSP inversion is applied to the high quality data processed by the erroneous SSP, the difference between the statistics from the original

surface and the one derived after the SSP inversion must be statistically insignificant. For this analysis, use is made of the histogram of the differences between the original footprints depth and those calculated after the SSP inversion. The surface difference can be calculated directly in QPS Qimera using the Surface Difference tool.

We also examine a data set that has a known refraction issue. The metric of success in this case is purely the reduction in the mean standard deviation of all the grid cells. For each grid cell, the standard deviation is computed as part of the gridding. In Qimera, we extract the standard deviation layer and examine the distribution both before and after the inversion exercise.

An important issue to investigate for both data sets is whether the application of the SSP inversion introduces unexpected features in the bottom topography. This means that for the parts where the refraction issue does not exist, the method should not change the bottom topography. To this end, the Qimera Slice Editor tool is used and the footprints for the small area without the refraction problem are compared before and after the application of the SSP inversion method.

Data Sets

For the assessment of the SSP inversion method, two data sets have been used. The first one is acquired by Rijkswaterstaat in the Nieuwe Waterweg which is a ship canal in the Netherlands from het Scheur (a branch of the Rhine-Meuse-Scheldt delta) west of the town of Maassluis to the North Sea at Hook of Holland. The data was was acquired in 19th of January 2010 using a Reson 8125 MBES and covers an area of 0.27 km^2 with water depths varying from 3.5 m to 26 m, shown in Figure 2. The survey area is characterized by a sandwave field which is traversing the sill plates of the Maeslantkering storm surge barrier (note the two arcuate features, roughly centered in the survey area). Vertical channel walls are also present. Oceanographic conditions in this area are estuarine with a pronounced salt wedge being the norm during various stages of the tide.

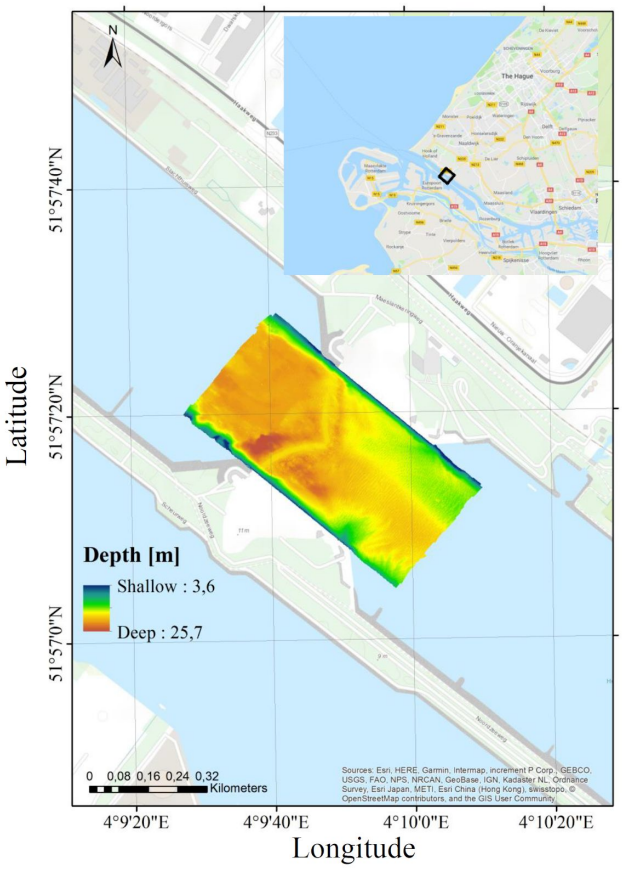

Figure 2. Bathymetry and location of the surveyed area (Nieuwe Waterweg, the Netherlands).

The dataset consists of 19 survey lines sailed parallel to each other with the distance between adjacent lines being approximately 20 m, providing overlap of ~70% between adjacent lines. As this dataset is of a very high quality we have used it to investigate the functionality of the SSP inversion algorithm.

The second data set considered in this contribution was acquired in the Bedford Basin, Halifax, Nova Scotia by a R2Sonic 2026 on 2nd of April 2017. The data was collected by R2Sonic with a pole-mount on a vessel of opportunity for engineering and testing purposes. It was later used as one of the primary data sets in R2Sonic's Multi-Spectral Challenge. The data covers an area of around 1.84 km^2 and consists of 13 track lines with approximately 50% survey overlap. The survey itself is small relative to the entire Bedford Basin. The basin is situated at the northwest end of Halifax Harbour and is blocked from full ocean circulation by a narrow sill. Typical oceanographic profiles indicate a two-layer structure with lower density surface water flowing outwards to the Atlantic Ocean, and deeper/denser water flowing into the Basin over the sill from the ocean.

Both initial surfaces contained a noticeable number of spikes which are to be cleaned. To this end, a spline filter was applied in QPS Qimera. After the application of the spline filter, there were some residual outlier soundings that were removed manually,

particularly in the Bedford Basin data set. The final Bedford Basin surface after removal of the spikes is shown in Figure 3, with the depths varying from 13 m to 89 m. One can see the refraction artefacts particularly in the northern part of the surveyed area. The objective is to apply the SSP inversion method to this data set and investigate to what extent the refraction issue will be corrected. Moreover, as this area has deep and shallow parts, non-parallel surveyed lines, and flat and rough topography, it is interesting to assess the performance of the inversion method in these different scenarios.

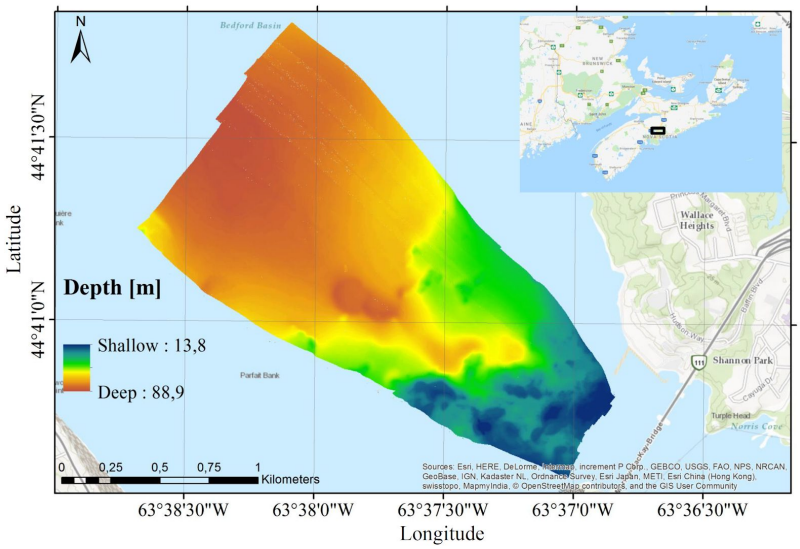

Figure 3. Bathymetry and location of the survey area (Bedford Basin, Halifax, Canada).

Results and Discussion

As mentioned, to assess the unbiasedness and the reproduction capability of the SSP inversion method, the data set acquired in Nieuwe Waterweg (by Rijkswaterstaat) was used. The erroneous SSP along with the four SSPs acquired during the survey are shown in Figure 4. The original data (in the format of .db file) was reprocessed assuming an erroneous sound speed profile and the standard deviation of the surface based on the measured and erroneous SSPs derived for a grid with the cell size of 0.5 m×0.5 m are shown in Figure 5(a and b). As expected the refraction artefacts appear and outer parts of the swaths exhibit a significantly larger standard deviation than the inner part.

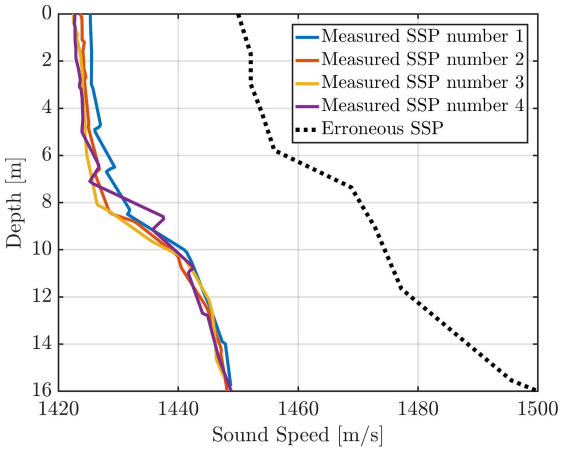

Figure 4. Four sound speed profiles that were measured during the survey (solid) and the erroneous sound speed profile introduced (dotted).

As mentioned, two approaches are available for SSP inversion in Qimera, i.e. Differential Evolution (DE) referred to as full search and Gauss Newton (GN) referred to as quick search. The DE is used to invert for the correct sound speed and correct the surface. Figure 5(c) shows the surface after applying the refraction correction. The comparison between the surfaces based on the measured SSPs and the one after SSP inversion, shows that the algorithm has successfully reconstructed the original surface (at least visually). It can also be seen that the standard deviation slightly decreased particularly for the area with the higher standard deviation in the middle of the surveyed area.

To assess the two surfaces (i.e. original and the one after application of DE) in more details, a small part of the surveyed area consisting of 30 consecutive pings is chosen, see the black rectangle in Figure 5. Figure 6 illustrates the footprint depth using the measured SSPs (a), erroneous SSP (b) and after application of the DE for SSP correction (c). It can be seen that the original footprints and the ones derived after SSP inversion are almost identical. This confirms that the DE SSP inversion does not manipulate the bottom topography and is able to reconstruct the original data.

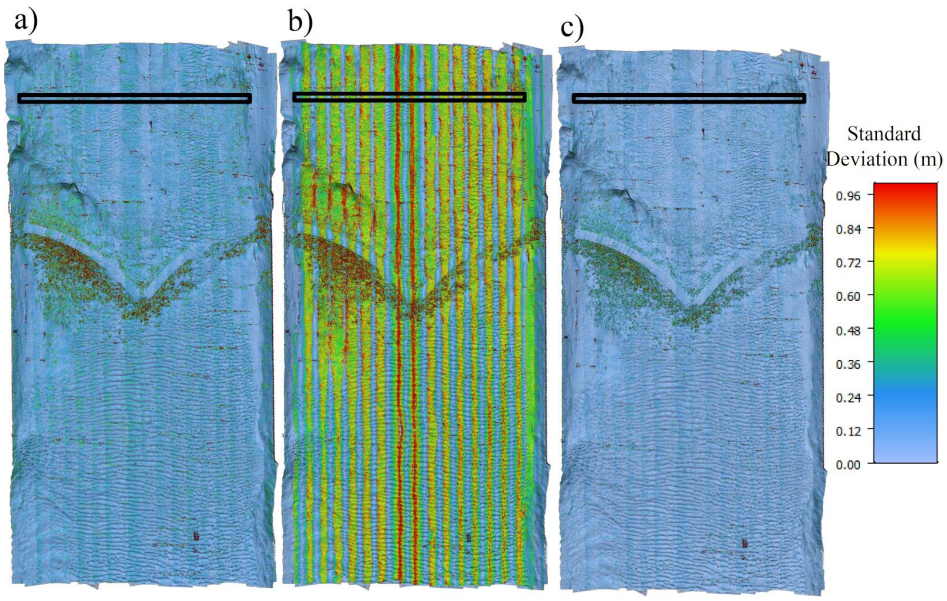

Figure 5. The standard deviation of the surfaces derived using the a) measured SSPs, b) erroneous SSP and c) results of the SSP inversion. The black rectangle identifies an area which will be assessed in further details.

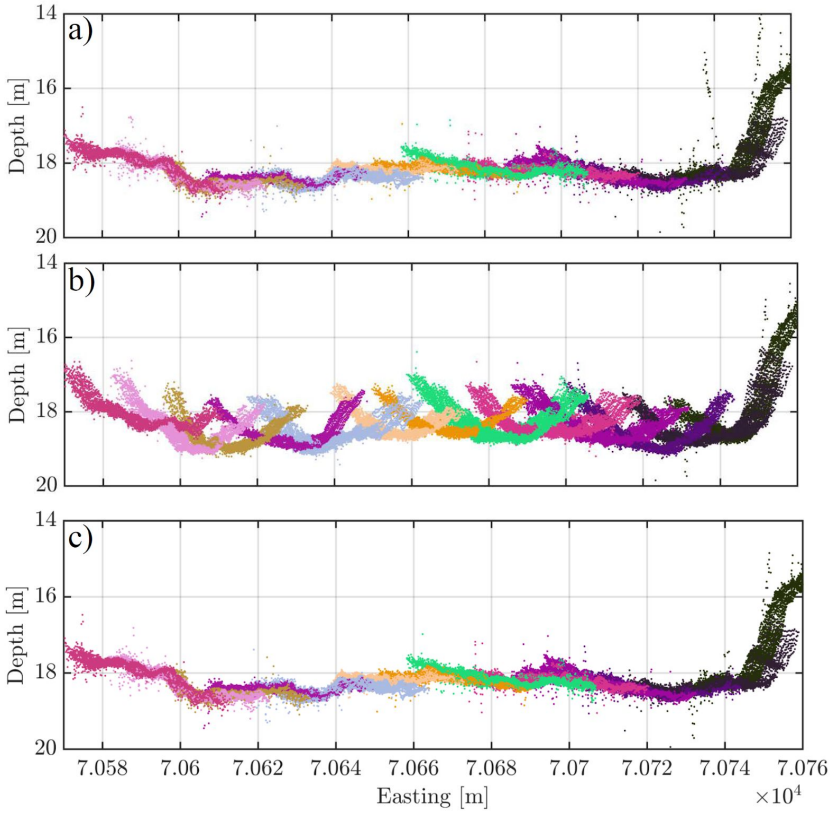

Figure 6. Footprints depth within the area consists of 30 pings shown by the black rectangle in Figure 4 using the a) original SSPs, b) erroneous SSP and c) results of the SSP inversion algorithm. Varying colors indicates different sailing tracks.

An important issue to assess is the statistics of the original surface and the one derived after SSP inversion, to ensure that the inversion does not introduce any appreciable depth bias. Presented in Figure 7 is the histogram of the differences between the two surfaces. For around 91% of the cells, the difference is between 0.000 m and 0.019 m. The mean and median of the differences are 0.004 m and 0.000 m, respectively, with the standard deviation of 0.030 m. The values for mean and median indicate that the SSP inversion method does not result in a biased estimate of the surface (the mean difference is not statistically significant at the 95% confidence level).

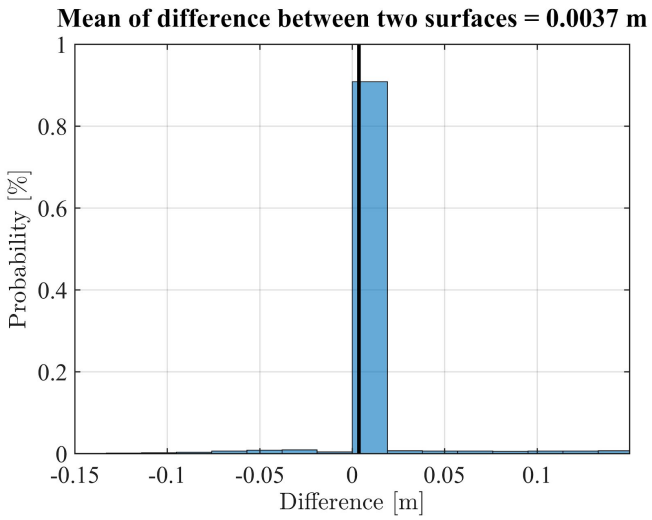

Figure 7. Histogram of the difference between the original surface and the one after SSP inversion.

As the next step, the SSP inversion method is applied to data with a refraction problem (see Figure 3). To highlight their presence, the map of the standard deviation is used instead of the bathymetry map. Figure 8(a) shows the standard deviation of the surface with the grid cell of the size 2 m× 2 m using the original measurements of the SSP. It is clear the refraction artefacts exist in the northern corner of the surveyed area. For convenience in presenting the results and making the comparisons easier, the surfaces are rotated to place them next to each other.

Applying the DE SSP inversion algorithm (“Full Search” in Qimera) and reprocessing the bathymetry using the new sound speed corrects for the the refraction issue observed to a large extent, as shown in Figure 8(b). The method also reduces the standard deviation in other parts where the refraction issue is less noticeable. Remaining sections of high standard deviation are due to the differences in bottom penetration of pings with varying frequency, seeing as this data was run in multi-spectral mode with the sonar frequency changing between 100 kHz, 200 kHz and 400 kHz on a ping-by-ping basis.

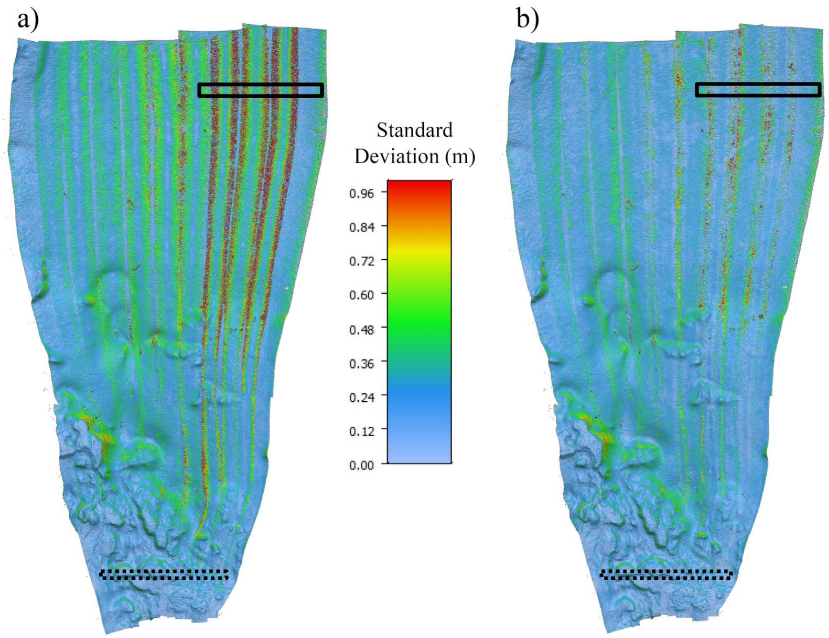

Figure 8. Standard deviation of the Bedford dataset based on the a) original SSP measurements and b) results of the SSP inversion. The black and dotted rectangles indicate areas which are investigated in more detail.

To analyse the statistics of both surfaces, the histograms of the standard deviation before and after the SSP inversion are presented in Figure 9 with light blue and red, respectively. It is seen that after the inversion the probability of having a smaller standard deviation is increased. The mean value of the standard deviation is also decreased by around 0.06 m (equal to the reduction in the median).

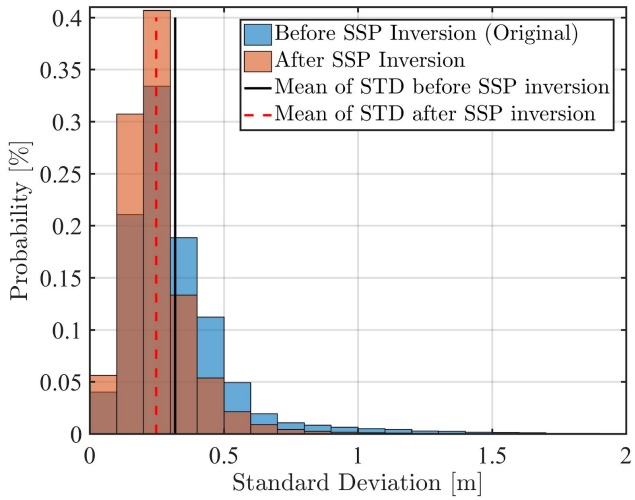

Figure 9. Histogram of the standard deviation of the original surface (blue) and the one after SSP inversion (light red). Shown with the solid black and dashed lines are the mean of the former and latter respectively.

To assess the two surfaces in more detail, two parts of the surveyed area consist of 30 and 10 pings with and without a refraction problem have been chosen, see the solid and dotted rectangles in Figure 8, respectively. Shown in Figure 10(a and b) are the footprints depth for an area with refraction problem indicated by solid rectangle in Figure 8 before and after the application of the DE inversion method. As can be seen, the method searches for the water column sound speeds that result in the maximum agreement in the depth along the overlapping parts of the swaths by minimizing the standard deviation of the depth measurements within the cells at the overlapping parts. Figure 11 illustrates the depth before and after inversion for the area shown by dotted rectangle in Figure 8, where the refraction problem does not exist. It is seen that the depth at the overlapping parts of the swaths are equal and hence the method does not change the footprint depths. This means that application of the method does not introduce artificial bathymetric features.

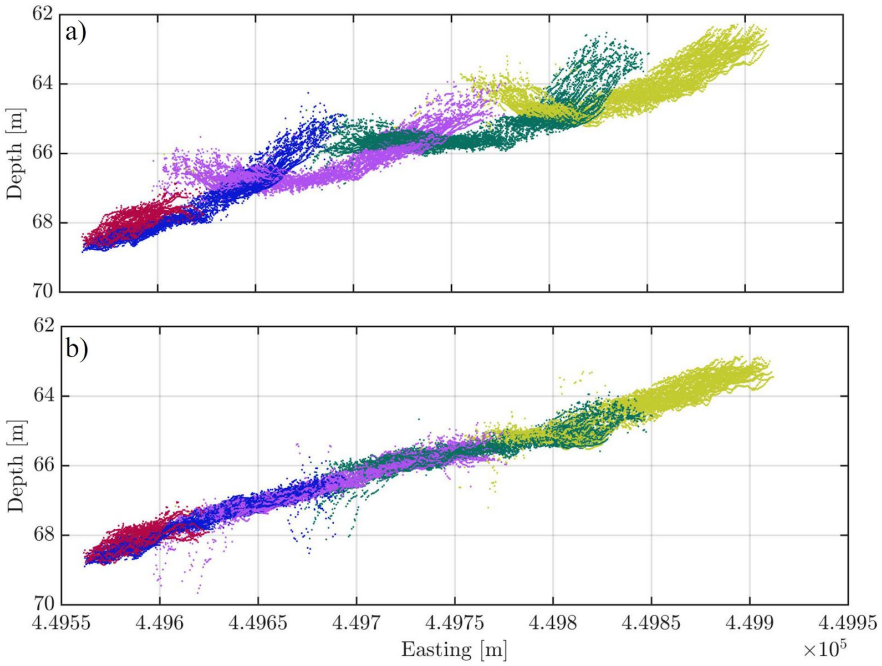

Figure 10. Footprint depths within the area consists of 30 pings shown by black solid rectangle in Figure 8 based the a) original SSPs and b) results of the SSP inversion algorithm. Varying colors indicate different sailing tracks.

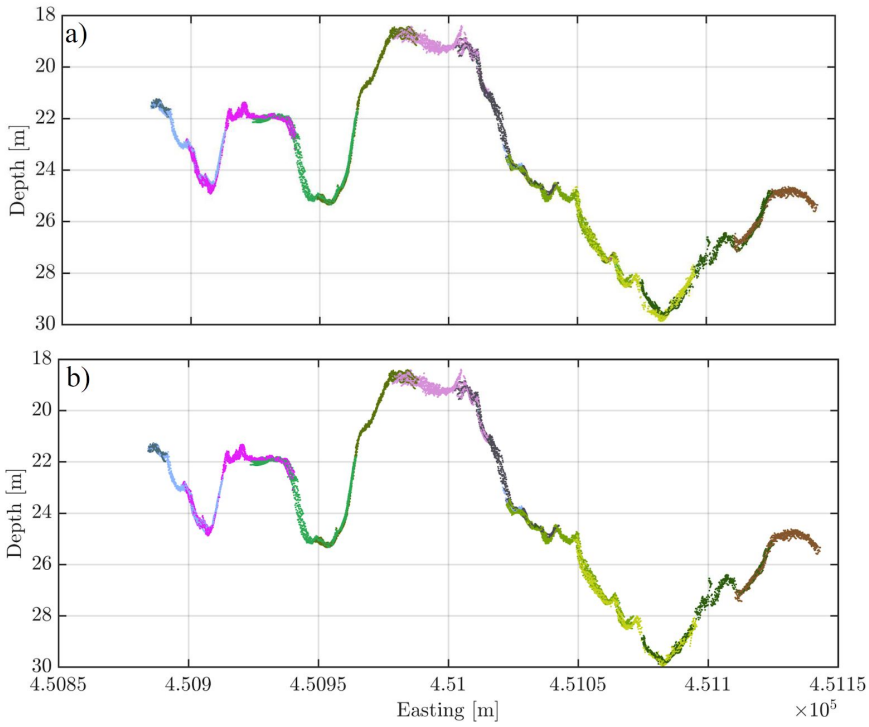

Figure 11. Footprint depths within the area consists of 10 pings shown by the black dotted rectangle in Fig. 8 based the a) original SSPs and b) results of the SSP inversion algorithm. Varying colors indicate different sailing tracks.

As mentioned in the previous section, the SSP inversion can be applied using either DE (Full Search) or Gauss Newton, GN, (Quick Search). The former is more powerful as it searches for the global minima as opposed to the latter in which its performance can deteriorate in case of converging to a local minima. Moreover, considering more complicated representations of the SSP in the water column (for further development and extension of the SSP inversion method implemented in Qimera) is more straightforward with DE than with GN as the former only requires updating the parameter space while the latter requires updating the observation equation and the Jacobian matrix. However, the GN has the advantage of being faster than DE by a factor varying from 3.3x to 5x.

As for the comparison between the performance of GN and DE, in case of a having a flat bottom and a clean dataset with limited number of outliers, both methods perform well and are able to correct the refraction problem (this has been confirmed based on both datasets). However, the presence of outliers complicates the situation. If the inversion results are smoothed (weighted mean), the deteriorating impact of outliers is mitigated. This is due to the nature of smoothing as is gives less weight to observations further from the mean. However, in case the results are not smoothed, the presence of outliers significantly deteriorates the performance of GN. Presented in Figure 12(a) is the standard deviation of the surface using the measured SSPs where the outliers and spikes are not removed (compare this surface to the one presented in Figure 8(a) where they are removed). The standard deviation is significantly higher than the surface based

on the clean data. Figure 12(b and c) shows the surfaces after SSP inversion using DE (Full Search) and GN (Quick Search) where the smoothing of the results is not carried out. It is seen that the performance of DE is noticeably superior to that of GN. GN also leads to an increase in the standard deviation of the surface in the parts where the outliers exist. The comparison between the surface based on the application of DE to the cleaned and uncleaned data (Figure 8a and Figure 12b) highlights the importance of the data cleaning step as it leads to a surface with much lower standard deviation. It is thus important to note that in case of having a noisy data set or dominant bottom topography, using GN is not recommended and DE is preferred (though it will take longer time to process).

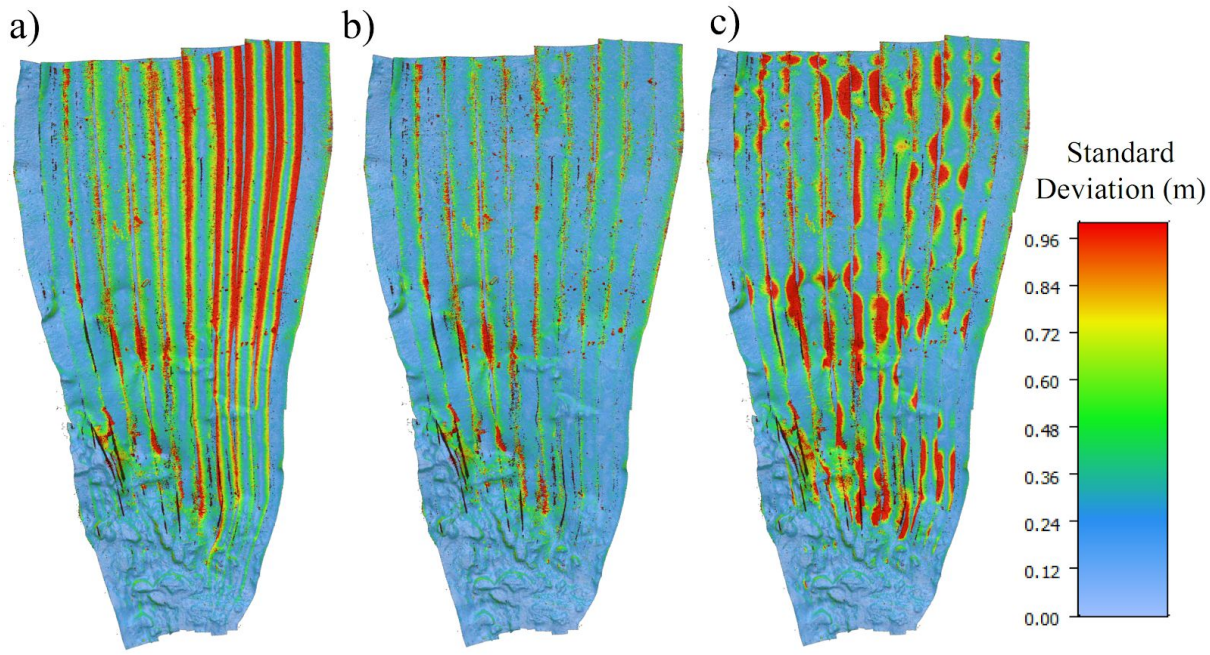

Figure 12. Standard deviation of the Bedford dataset based on the a) DE SSP inversion and b) GN SSP inversion without smoothing the results and removing the outliers.

SUMMARY AND CONCLUSION

In this paper, we have explained the basic approach taken to minimize bathymetry data artifacts that are due to oceanographic variability in sound speeds. We have examined two case studies briefly, in an effort to demonstrate that the proposed method does not introduce bias and that it successfully improves data quality. This was demonstrated for two data sets, one of which was simulated to have refraction problems and the second of which suffered from true artifacts. It is hoped that the analysis methods used to evaluate the two data sets show how end users can assess for themselves the impact of the inversion methods such that they can do their own investigations into when it is acceptable to use the inversion method. We look forward to hearing from end users about the successes and failures of the inversion method in a variety of oceanographic

environments, differing seafloor morphology and finally over a range of survey line design strategies.

REFERENCES

Ding, J. , Zhou, X., and Q. Tang (2008). A method for the removal of ray refraction effects in multibeam echo sounder systems. Journal of Ocean University of China, 7(2): 233–236.

Kammerer, E. and J.E. Hughes Clarke (2000). new method for the removal of refraction artifacts in multibeam echosounder systems. In Canadian Hydrographic Conference Montréal.

Mohammadloo, T.H., Snellen, M., Simons, D.G., Renoud, W. and J. Beaudoin (2018). Compensation of multibeam echosounder bathymetric measurements for errors due to the unknown water column sound speed, in preparation.

Olver, P.J. (2016). Introduction to Partial Differential Equations (Undergraduate Texts in Mathematics). Springer. ISBN 978-3-319-02098-3.

Price, K. and R. Storn (1995). Differential evolution-a simple and efficient adaptive scheme for global optimization over continuous space. Technical Report, International Computer Science Institute.

Snellen, M. and D. G. Simons (2008). An assessment of the performance of global optimization methods for geo-acoustic inversion. Journal of Computational Acoustics, 16(02):199–223.

Snellen, M., Siemes, K. and D. G. Simons (2009). A model-based method for reducing the sound speed induced errors in multi-beam echo-sounder bathymetric measurements. *OCEANS 2009 - EUROPE*, pp. 1-7.

Teunissen, P.J.G (2000). Adjustment Theory: an introduction (Mathematical Geodesy and Positioning). VSSD. ISBN 90-407-1974-8.

ACKNOWLEDGEMENTS

We would like to thank both Rijkswaterstaat and R2Sonic for their permission to use their data sets for this evaluation.